Yeast-based High-throughput Screening of *Plasmodium falciparum* Phosphodiesterase Beta (PDEβ) for Malaria Drug Discovery

Kah Shuen Gan

Under the direction of
Dr. Charles Hoffman
Boston College

Research Science Institute
August 1, 2023

Abstract

Malaria is an infectious disease that continues to be the leading cause of death in developing countries. The emergence of drug-resistant *Plasmodium falciparum* parasite, which causes the most severe and lethal malaria, poses a significant challenge to disease eradication efforts and necessitates the discovery of new drug targets. This study focuses on the cyclic nucleotide signaling pathway in *P. falciparum*, specifically, the action of the enzyme phosphodiesterase beta (PfPDEβ). PfPDEβ catalyzes the hydrolysis of intracellular second messenger 3',5'-cyclic adenosine monophosphate (cAMP), a key regulator of *P. falciparum* asexual blood stage development. I successfully cloned the PfPDEβ gene and constructed *Schizosaccharomyces pombe* yeast strains expressing PfPDEβ. A yeast-based high-throughput screen (HTS) was developed and optimized to identify PfPDEβ inhibitors. 162 known mammalian phosphodiesterase (PDE) inhibitors were screened and the growth response of the yeast strains expressing PfPDEβ was analyzed. Six hit compounds, namely BC8-8, BC8-19, BC8-20, BC11-29, BC40, and BC42, were identified as PfPDEβ inhibitors. This study has successfully developed a chemical toolkit to assess the utility of PfPDEβ as a drug target, advancing ongoing efforts in antimalarial drug development.

Summary

Malaria is the leading cause of death in developing countries, with the *Plasmodium falciparum* parasite being the primary cause of severe and lethal forms of this infectious disease. Although antimalarial drugs have been developed and used to treat malaria over the past decade, the emergence of drug-resistant parasites has reduced the efficacy of these drugs. Hence, there is an urgent need to discover new drug targets to eradicate the disease. This study focuses on a specific pathway in the parasite called the cyclic nucleotide signaling pathway. I studied an enzyme called phosphodiesterase beta (PfPDEβ) which plays a crucial role in the development of the parasite. A cost-effective, time-efficient and robust yeast-based screening platform was optimized to identify compounds that could inhibit the PfPDEβ enzyme. I have successfully developed a toolkit to assess the potential of PfPDEβ as a drug target, bringing us closer to developing novel antimalarial drugs.

1 Introduction

Malaria is a life-threatening disease transmitted to humans by a female Anopheles mosquito that is infected with apicomplexan parasites of the *Plasmodium* genus [1]. According to the World Health Organization (WHO), 247 million cases and 619,000 deaths were reported globally in 2021, mostly from Africa and South-East Asia [2]. Of the five human malaria parasite species, *Plasmodium falciparum* is the most lethal, responsible for 90% of the world's malaria mortality [3], due to its cytoadherence and sequestration abilities that allow it to evade the host's immune system and intensify the severity of the disease [4]. For the past two decades, artemisinin-based combination therapies (ACTs), which work by poisoning essential malaria proteins, have been an effective primary treatment for *P. falciparum* [5]. However, the emergence and spread of drug-resistant *P. falciparum* worldwide have compromised the efficacy of all ACTs currently recommended by WHO [6, 7, 8, 9], exacerbating the morbidity and mortality of future malaria epidemics [5]. Hence, there is a pressing need to identify potential drug targets as well as screen for compounds that could be developed into novel drugs.

Cyclic nucleotide phosphodiesterases (PDEs) are promising targets for such therapeutics, due to their critical role in regulating the *P. falciparum*'s life cycle, which consists of two stages that are tightly controlled by cyclic nucleotide signaling, as illustrated in Supp. Figure 1. (1) The asexual blood stage is responsible for disease pathology and symptoms. (2) The sexual stage, called gametogenesis, is responsible for the transmission of the parasite. Levels of second messenger 3',5'-cyclic adenosine monophosphate (cAMP) and 3',5'-cyclic guanosine monophosphate (cGMP) regulate these cellular functions. When cAMP and cGMP reach a concentration threshold, they activate cAMP-dependent protein kinase (PKA) and cGMP-dependent protein kinase (PKG), respectively [10, 11]. PDEs, which hydrolyze cAMP and cGMP, reduce PKA and PKG activity, facilitating sporozoite motility and invasion [11], blood stage invasion and growth [12] and cell cycle control [13], as well as gametogenesis [14], ookinete differentiation and motility [15], respectively.

PDEs' ability to regulate PKA and PKG activity to a high degree of specificity has led to a growing interest in inhibitors of PDEs as promising therapeutics. Presently, PDE inhibition is well established and has been used in various disease treatments, including pulmonary arterial hypertension and erectile dysfunction [16, 17]. Each PDE has a unique 3-dimensional active site which presents an opportunity for the development of high-affinity competitive inhibitors that can increase and dysregulate PKA and PKG activity by accumulating cAMP and cGMP, respectively [18]. In the context of malaria, the *P. falciparum* genome encodes four PDEs (PfPDEα, PfPDEβ, PfPDEδ and PfPDEγ), among which, PfPDEβ is the master regulator of cAMP signaling in schizogony and asexual blood stage development [10, 11]. In constrast, PfPDEα, PfPDEδ and PfPDEγ are not essential for blood stage replication and invasion, as seen in Supp. Figure 1 [15, 19, 20]. Therefore, inhibiting PfPDEβ has great potential to reduce *P. falciparum* development in humans and thus impede malaria transmission. This is especially true because PfPDEβ exhibits distinct sequences from human PDEs (HsPDEs), enabling greater therapeutic specificity. Using the Protein Basic Local Alignment Search Tool (BLASTP) search, I found that the amino acid sequence of PfPDEβ is significantly different from that of HsPDEs. Specifically, amino acids of PfPDEβ are only 35% identical and 49% similar to HsPDE1A (Supp. Figure 2a) and 35% identical and 54% similar to HsPDE9A (Supp. Figure 2b). On top of this variation, using Clustal Omega (a multiple sequence alignment program), I found that PfPDEβ does not align with 3 of the 18 invariant amino acids in HsPDEs (Supp. Figure 3). This highlights the significant differences between the primary structure of the active site of PfPDEβ and HsPDEs, which enable the development of highly selective PfPDEβ inhibitors that target specific signaling pathways for malaria treatment without disrupting human cellular functions. Hence, PfPDEβ is a promising drug target. At present, studies have shown the therapeutic effects of knocking out the PfPDEβ gene in *P. falciparum* through gene deletion [21]. However, there is a gap in demonstrating that PfPDEβ inhibition by small molecules could be a viable method to treat malaria.

This study differentiates itself from current drug discovery efforts as it uses a yeast-based screening approach. At present, drug development has been largely dominated by pharmaceutical companies that rely on two primary methods to identify potential drug compounds. Firstly, biochemical screening with *in vitro* enzyme assays is used to identify compounds that interact with target PDEs directly. However, this process has its limitations including difficulties in prioritizing compound efficacy due to insufficient information [22], potential ineffectiveness of compound in *P. falciparum* that requires further medicinal chemistry to increase cell permeability, and high costs needed to purify PDE targets and carry out assays [23, 24]. Secondly, phenotypic screening with target organisms is employed to identify cell-permeable potential drug compounds. However, difficulty in identifying the targeted protein hinders our understanding of the action of the drug and there may be issues in culturing the organism [23, 24]. In contrast, this study utilizes a *Schizosaccharomyces pombe* yeast-based HTS approach to identify cell-permeable compounds in a more cost-effective manner [25]. *S. pombe* has been found to regulate metabolism and sexual development through a glucose-sensing cAMP pathway [26] and is an ideal medium for screening for several reasons. Firstly, being a single-celled organism facilitates the growth of simple mutant phenotypes in microtiter dishes. Secondly, as a eukaryote, *S. pombe* undergoes many similar biological processes to human cells [27]. Thirdly, *S. pombe*'s ability to support autonomously-replicating plasmids and undergo homologous recombination enables the construction of screening and counter-screening strains, essential for gene cloning purposes [28].

This study aims to develop a chemical toolkit to assess the potential of PfPDEβ as an antimalarial drug target through a yeast-based screening platform. To achieve this goal, compound screening conditions were optimized and a screen of 162 compounds was carried out to identify and characterize potential PfPDEβ inhibitors. It is important to note that in this study, the screening of compounds is not intended to identify potential malaria drug compounds directly. Instead, the goal is to identify compounds that could be used in whole *P. falciparum* parasite screening to assess the impact of inhibiting PfPDEβ. Subsequently, these

inhibitors could be further studied to justify pursuing High Throughput Screening (HTS) on PfPDEβ. As such, this study paves the way for the development of novel antimalarial drugs.

2 Methods

2.1 Strains, media and general techniques

Yeast strains used are listed in Table 1. Host strains CHP1236 and CHP1247 were used to express PfPDEβ via the construction of strains GKS1 and GKS2. Oligonucleotides used for Polymerase Chain Reaction (PCR) and DNA sequencing are listed in Supp. Table 1. Edinburgh Minimal Medium (EMM) and Yeast extract medium (YES) were used as growth media. EMM-lys medium (EMM lacking lysine) was used to select cells that produced lysine due to the acquisition of plasmid pJVI or pJVI-PfPDEβ.

Strain	**Genotype**	**Phenotype**
CHP1236	*h- fbp1::ura4 ura4::fbp1-lacZ leu1-32 his7-366 pap1Δ::ura4- cgs2-2 lys2-97 git2-2::his7+*	No cAMP production No PDE activity
CHP1247	*h+ fbp1::ura4 ura4::fbp1-lacZ leu1-32 pap1Δ::ura4- cgs2-2 lys2-97 11his3-Δ1 gpa2Δ::his3+*	Low cAMP production No PDE activity
GKS1	*h- fbp1::ura4 ura4::fbp1-lacZ leu1-32 his7-366 pap1Δ::ura4- cgs2-2 lys2-97 git2-2::his7+* [pJVI-PfPDEβ]	No cAMP production PfPDEβ activity
GKS2	*h+ fbp1::ura4 ura4::fbp1-lacZ leu1-32 pap1Δ::ura4- cgs2-2 lys2-97 11his3-Δ1 gpa2Δ::his3+* [pJVI-PfPDEβ]	Low cAMP production PfPDEβ activity

Table 1: Yeast strains used in this study.

2.2 Acquisition of open-reading frame

The PfPDEβ protein sequence was obtained through an NCBI protein search. Using BLASTP, the PfPDEβ protein sequence was aligned with *Homo sapiens* proteins to identify the protein sequence coding for the catalytic domain. To optimize the DNA sequence for

S. pombe, codon optimization was performed using the Codon Optimization Tool from Integrated DNA Technologies. DNA sequences upstream and downstream of a unique *Sac*II site in pJVI were added to the ends of the DNA sequence to facilitate homologous recombination. DNA was synthesised by Twist Bioscience.

2.3 Plasmid transformation and rescue in *S. pombe*

S. pombe strains CHP1236 and CHP1247 were transformed with *Sac*II-linearized plasmid pJV1 and the PfPDEβ gene, using the Dimethyl sulfoxide (DMSO) Transformation protocol, as described in Hill *et al.* [29]. Details in Appendix A.5. Plasmids were isolated from yeast transformants using the Smash and Grab technique, as described in Hoffman *et al.* [30]. Details in Appendix A.6.

2.4 Plasmid preparation

Plasmids in *E.coli* transformants were purified using the QIAgen Spin Column Kit protocol with the following modifications. Before pelleting, *E.coli* was grown as a *E.coli* lawn on an LB ampicillin plate, instead of an LB liquid. Pellet was resuspended in 220μl, instead of 250μl, of buffer P1. Plasmids were incubated in a water bath at 65℃, instead of room temperature. 500ng of plasmid was transferred to tubes containing 0.5μl *Pst*I or *Pvu*II from New England Biolabs. 2μl 10x buffer 3.1r and sterile water were added to bring volume to 20μl. The tubes were incubated at 37℃. Gel electrophoresis was carried out on *Pvu*II digested plasmid using 1% agarose gel in TAE buffer. The uncut plasmid was diluted with sterile water to form a 20μl solution with 200ng/μl DNA concentration and sent to Eton Bioscience for DNA sequencing using primers Tif-rev and ura5-seq (Supp. Table 1). *Pst*I cut plasmid was used for integrative plasmid transformation of CHP1236 and CHP1247 to construct strains GKS1 and GKS2, respectively.

2.5 Selection of strains with integrated plasmids

Replica plating

S. pombe strains CHP1236 and CHP1247 were transformed to Lys^+ to construct strains GKS1 and GKS2, respectively. EMM-lys transformation plates were incubated at 30℃ for three (GKS2) and four (GKS1) days respectively. Then, three rounds of replica plating of transformants were carried out on YES plates (with one-day incubation at 30℃ between each round) and finally plated onto an EMM-lys plate [31]. Stable integrants displayed Lys^+ growth after one-day incubation at 30℃. Integrants could be selected because the integrated plasmids replicated along with the yeast's chromosome and were maintained during mitosis, whereas, colonies of transformants carrying autonomously replicating plasmids consisted of mostly Lys^- cells due to plasmid loss during mitosis.

Tetrad dissector

CHP1236 and CHP1247 transformant plates were examined for colonies after three days of incubation at 30℃. Larger colonies, indicative of integrated plasmids as observed by Charles Hoffman, were picked using a tetrad dissector and placed on a YES plate. After one day, the cells were spread out on the same YES plate to facilitate growth. The next day, cells were plated onto an EMM-lys plate. The plates were examined on a tetrad dissector to determine whether any transformants contained only Lys^+ cells, indicating plasmid integration.

2.6 Cell length response to exogenous cyclic nucleotides (cNMPs)

Strain GKS1 and CHP1236 host strain (no PDE) were transferred into separate 2ml EMM cultures. 0.2ml of cells were transferred into nine small culture tubes containing 0.8ml of EMM with no cNMP, EMM+156.25μM cAMP, EMM+312.5μM cAMP, EMM+625μM cAMP, EMM+1250μM cAMP, EMM+156.25μM cGMP, EMM+312.5μM cGMP, EMM+625μM

cGMP, EMM+1250μM cGMP respectively. Cells were incubated at 30℃ for three hours. Cell length was analyzed using oil microscopy and the Fiji software.

2.7 Screening conditions

For cNMP Profiling of PDEs, 10μl of 5FOA medium (0.4g/L 5FOA + either 2.5mM of cAMP or cGMP) was pipetted into a 384-well microtiter plate. Cell cultures were diluted into 1.4ml 5FOA (no cNMP) to 10^5 cells/ml. 40μl of cell culture (CHP1236 or GKS1) was added to nine empty wells, and then wells containing cAMP or cGMP, followed by two-fold serial dilutions to carry out a dose responses curve. For optimization of screening conditions and screening for PfPDEβ inhibitors, 9μl of 5FOA medium (GKS1: 0.5g/L 5FOA + 12.5μM cAMP, GKS2: 0.5g/L 5FOA) and 1μl of DMSO or 5mM compound were pipetted into a 384-well microtiter plate. The 162 compounds screened in this study are listed in Supp. Table 2. 40μl cell culture (GKS1 or GKS2) at a cell density of 2.5×10^4 or 5×10^4 was added to six empty wells, then to the compound-containing well, followed by two-fold serial dilutions. Cultures were incubated at 30℃ for 48 hours. Optical density (OD) readings of cultures were measured using a microplate reader. The chemical structures of hit compounds were found using NovoPro Labs SMILES to Structure software. The similarity of the chemical structure of hit compounds was analyzed using the Tanimoto coefficient, the ratio of the number of common features to the total number of features [32], using RDKit in Python.

3 Results

3.1 Successful cloning of PfPDEβ gene

A plasmid, pJVI-PfPDEβ, encoding the catalytic domain of the PfPDEβ protein was successfully constructed via gap repair-transformation [33]. Subsequent transformation of the recombinant plasmid, carrying the PfPDEβ gene, into *S. pombe*, as outlined in Section 2.2 and Section 2.3, was successful, as verified in Figure 1a. Plasmid purification and

preparation, as described in Section 2.4, were performed on DNA from *E.coli*. To verify the successful insertion of PfPDEβ into the plasmid, restriction digestion with *Pvu*II was carried out. The results from gel electrophoresis verified that PfPDEβ was successfully inserted into the plasmid, as the observed DNA length corresponded to the expected length of segments (2.0kb and 6.8kb) determined using NEBcutter V2.0, as shown in Figure 1b. Successful insertion of PfPDEβ catalytic domain into insert was further confirmed using DNA sequencing and Basic Local Alignment Search Tool (BLAST).

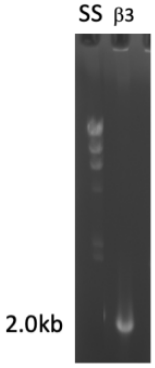

(a) PCR product of transformants have a length of 2.0kb, corresponding to the length of the open reading frame.

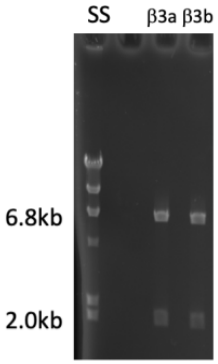

(b) Plasmid after restriction digestion with *Pvu*II. 2.0kb and 6.8kb DNA segments were observed for both candidates (β3a and β3b).

Figure 1: Gel electrophoresis Image of Plasmid DNA.

3.2 Successful construction of strains to find integrated plasmids

Transformation of integrated plasmids into yeast strains

Strains expressing PfPDEβ with the *fbp1-ura4* reporter were constructed, such that Ura4 activity reflects PfPDEβ activity, enabling the screening for PDE inhibitors using a 5FOA assay with the following screening pathway. In the presence of PfPDEβ, cAMP levels are reduced, leading to low PKA activity which derepresses *fbp1-ura4* reporter transcription. These cells express *ura4* and grow on medium lacking uracil (SC-ura) but are 5-fluoro-orotic acid (5FOA) sensitive and unable to grow on 5FOA medium (Figure 2a). In contrast, when PfPDEβ is inhibited by hit compounds, cAMP levels rise, leading to high PKA activity,

which represses *fbp1-ura4* reporter transcription. These cells are unable to grow on SC-ura but are 5FOA-resistant and grow on 5FOA medium (Figure 2b) [27]. By measuring growth using OD, compounds that inhibit PfPDEβ can be identified [25]. To construct the strains that express PfPDEβ, plasmid DNA was subjected to restriction digestion using *Pst*I to cut the *lys2* gene, resulting in linearized plasmids. The linearized plasmids were targeted for homologous recombination to the *lys2* locus for transformation into yeast strains CHP1236 and CHP1247, constructing strains GKS1 and GKS2, respectively.

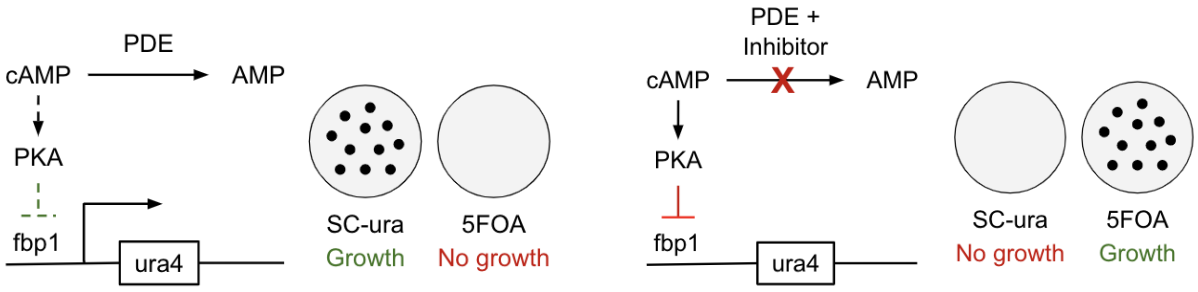

(a) Pathway and expected phenotype in the absence of PDE inhibitor.

(b) Pathway and expected phenotype in the presence of PDE inhibitor.

Figure 2: Schematic diagram of cAMP pathway that regulates *fbp1-ura4* reporter in *S. pombe*.

Selection of strains with integrated plasmids

Strains with integrated plasmids were identified using both the traditional replica plating and tetrad dissector methods, as outlined in Section 2.5. The tetrad dissector approach expedited the process by one day. GKS1 and GKS2 integrants were obtained, as illustrated in Figure 3.

3.3 Characterization of PfPDEβ using 5FOA assay

Determination of pre-growth conditions for yeast strains

Prior to performing the 5FOA screening, the optimal amount of cNMPs needed to activate PKA was determined. This was necessary to inhibit *ura4* gene expression, making

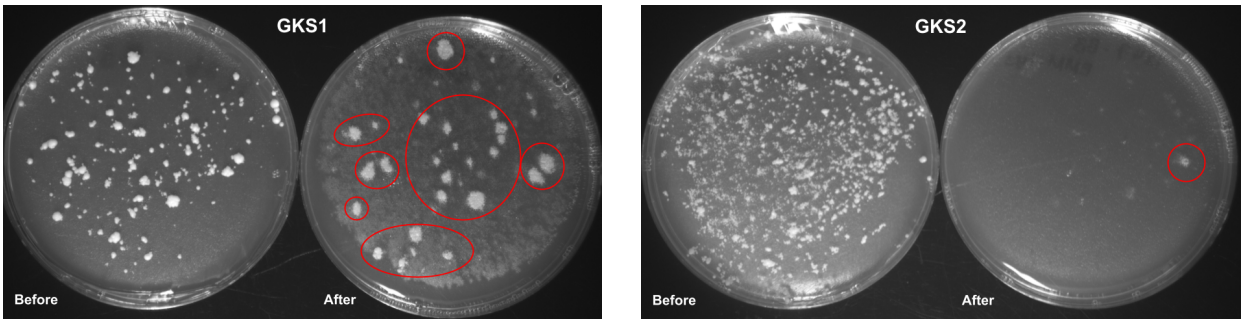

(a) Strain GKS1. **(b)** Strain GKS2.

Figure 3: Identification of transformants carrying integrated plasmids by plasmid loss. Left EMM-lys plate shows strains before replica plating, carrying both integrated and autonomously replicating plasmids. Right EMM-lys plate shows strains after replica plating, carrying only integrated plasmids.

the strains 5FOA-resistant before screening, such that 5FOA-resistant growth could be attributed to the hydrolysis of cNMPs by PfPDEβ. Hence, during the pre-growth of the strains, various amounts of cNMPs were introduced to enhance PKA activity and repress the *fbp1-ura4* reporter. Since an increase in PKA activity can be observed by an increase in cell length [34], cell length was used to determine the amount of exogenous cNMPs needed for PKA activation. Upon supplementing the GKS1 strain with 125μM cAMP, a notable increase in cell length of +5.5μM was observed, as seen in Figure 4. This indicated that PKA was activated, validating that these specific cNMP amounts were suitable pre-growth supplements for the yeast strains.

Optimization of screening conditions

cNMP profiling was performed to understand the hydrolytic activity of PfPDEβ and optimize screening conditions. The activity of PfPDEβ was studied using the yeast-based 5FOA assay, as outlined in Figure 2. When screening GKS2, which produces some cAMP, no exogenous cNMPs were added to the 5FOA medium, as PKA activity and *fbp1-ura4* reporter repression could be regulated by the cAMP produced by GKS2. On the other hand, when screening GKS1, which produces no cAMP, exogenous cNMPs needed to be added to the 5FOA medium to regulate PKA activity and *fbp1-ura4* reporter repression. This is because

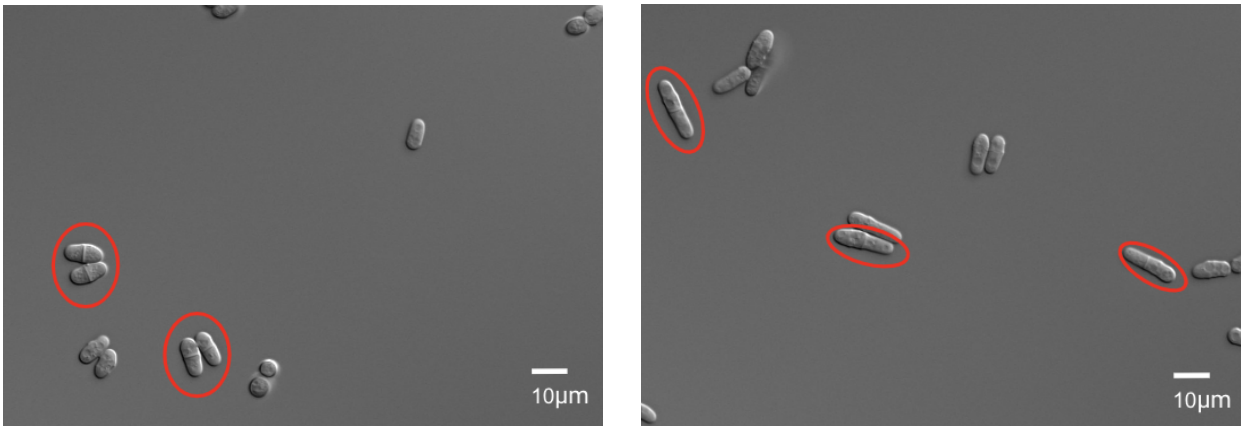

(a) No cAMP added. Length = 9.24µM. **(b)** 125μM cAMP added. Length = 14.74µM.

Figure 4: 125μM cAMP activated PKA in strain GKS1, as seen by the notable increase in the average length of cells with a fission plate (same stage of the cell cycle).

the lack of cAMP production in the GKS1 strain causes the cells to express the *ura4* gene and be 5FOA sensitive. However, the Ura4 proteins would have interfered with the analysis of the effects of PDE inhibitors in the 5FOA assay. Hence, exogenous cNMPs were added to test the cell's ability to maintain 5FOA-resistance rather than confer 5FOA-resistance. The amount of cAMP and cGMP needed for the cell to express 5FOA-resistance was determined, as described in Section 2.7. Upon the expression of PfPDEβ, the amount of cAMP needed to achieve 5FOA-resistance increased while the amount of cGMP remained relatively constant, as shown by the shift of the blue curves when PfPDEβ was present in Figure 5. This suggests that PfPDEβ hydrolyzes cAMP, but not cGMP. Hence, 12.5μM cAMP was added to the 5FOA medium for GKS1 strains, increasing PKA activity to repress the *fbp1-ura4* reporter such that cells confer 5FOA-resistance.

To further optimize 5FOA assay screening conditions, pilot screenings of compound collection 8 using different conditions were conducted, as detailed in Section 2.7. To determine the optimal yeast strain, assays were performed using strains GKS1 and GKS2, where strain GKS1 was ultimately selected for future screens. This was because strain GKS1 showed a more pronounced distinction in growth between DMSO (the solvent used to dissolve the compounds, thus serving as a vehicle control) and compounds, as seen in Figure 6, enabling

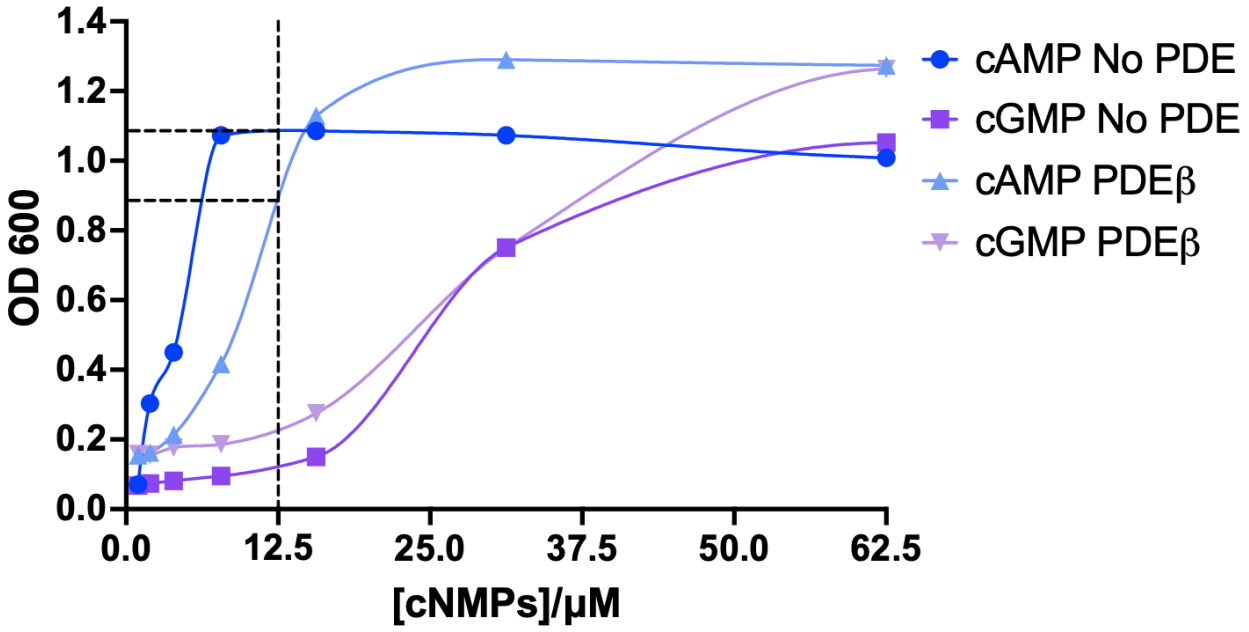

Figure 5: cNMP dose-response curve of strains CHP1236 (no PDE) and GKS1 (PfPDEβ). The optimal amount of cAMPs to be added to observe 5FOA growth in the presence of PfPDEβ is 12.5μM. 0.4g/L 5FOA was used in this assay. Subsequent assays used 0.5g/L 5FOA to further reduce growth of cells exposed to 12.5μM cAMP.

clearer analysis, as cell growth could be predominantly attributed to compounds inhibiting PfPDEβ. Additionally, optimization was carried out for 5FOA concentration (0.4g/L and 0.5g/L) and cell density (2.5×10^4 cells/ml and 5×10^4 cells/ml) (data not shown). Based on the results, the optimal screening conditions were determined to be using strain GKS1 with a cell density of 5×10^4 cells/ml in 0.5g/L 5FOA with 12.5μM cAMP supplement.

3.4 Identification of PfPDEβ inhibitors through HTS screening

In the genetically engineered yeast strain, GKS1, a frameshift mutation in the *cgs2* PDE gene effectively disrupts *S. pombe* PDE activity. Hence, the PDE activity observed in the experiments is solely attributed to PfPDEβ. 5FOA screening relies on the 5FOA growth phenotype, which is expressed by transcription of the *fbp1-ura4* reporter. In the presence of PfPDEβ inhibitors, GKS1 strains should confer 5FOA-resistant growth, as PfPDEβ inhibitors increase cAMP levels to repress *fbp1-ura4* transcription (Figure 2b). The screening

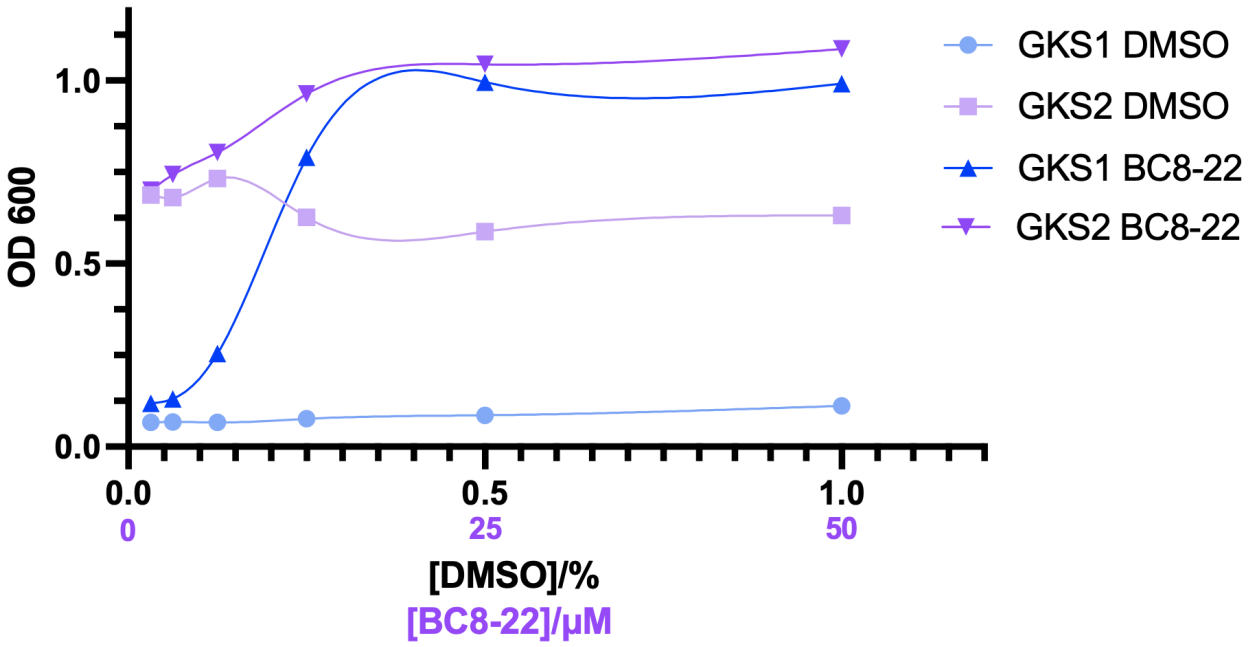

Figure 6: Dose-response curve of strains GKS1 and GKS2 using DMSO (control) and BC8-22 (a hit compound identified in collection 8). Greater difference in growth between DMSO and BC8-22 was observed when strain GKS1 was used.

was performed using 162 compounds previously identified as HsPDE inhibitors, as described in Section 2.7 and Section 3.3 [35, 36, 37, 38, 39]. From this initial screening, 42 potential hit compounds that resulted in the greatest increase in OD, as listed in Supp. Table 3, were selected. Focused screening on these 42 compounds was performed in triplicate. Hit compounds were identified by their ability to increase OD compared to the control (DMSO) to a statistically significant extent. The increase in OD was determined by calculating the ratio of OD with the compound added to the OD with only DMSO. Six hit compounds, namely BC8-8, BC8-19, BC8-20, BC11-29, BC40, and BC42, were identified as significant hits based on an upper-tailed one-sample t-test with null hypothesis OD ratio ≤ 1, followed by multiple hypothesis test correction via the Benjamini–Hochberg procedure ($q = 0.1$) [40]. Hit compounds were analyzed in a dose-response curve and half-maximal effective concentration (EC_{50}) values were determined, as illustrated in Figure 7. These compounds effectively inhibited PfPDEβ and reduced its hydrolytic activity, leading to an accumulation of cAMP and increased PKA activity. Consequently, the *fbp1-ura4* reporter was repressed, resulting

in strains exhibiting 5FOA-resistant growth. BC8-20 stood out as the strongest and most potent inhibitor of PfPDEβ. It demonstrated the greatest increase in OD and displayed the lowest EC_{50} value of 0.295μM, as seen in Figure 7. This suggests that even at low concentrations, BC8-20 effectively inhibited PfPDEβ, making it a highly potent compound and promising lead compound for further screening.

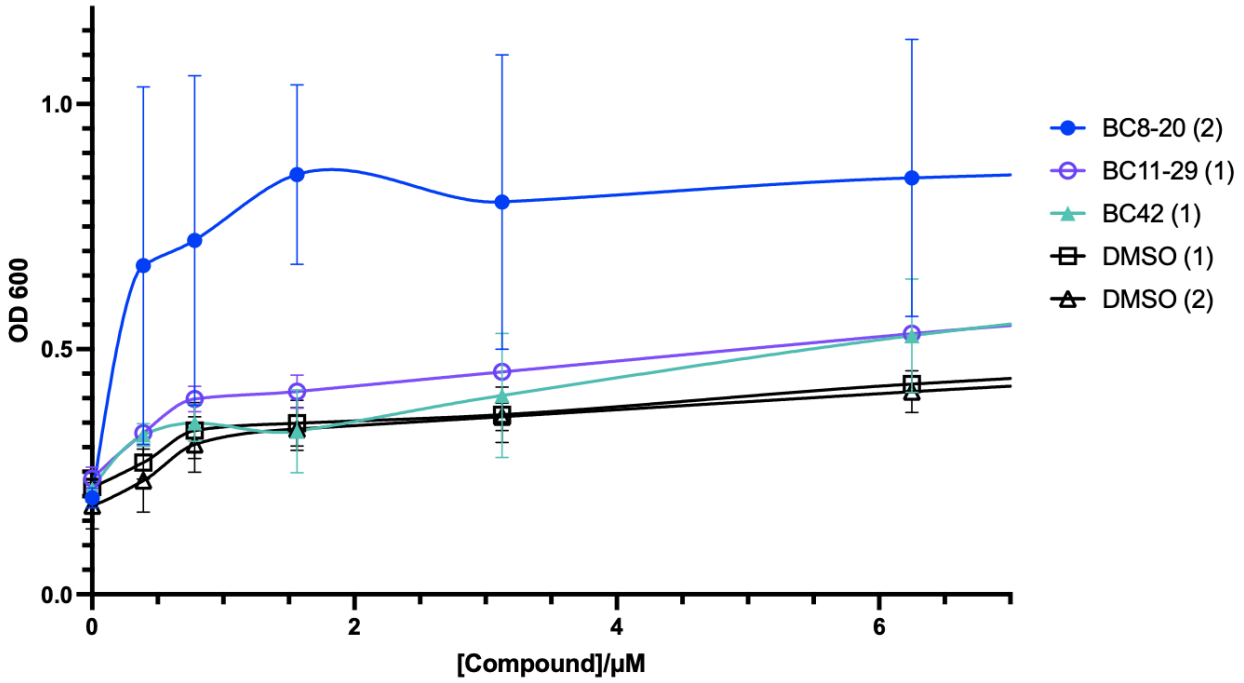

Figure 7: Dose-response curve of average OD values of three duplicate wells against the concentration of the top three hit compounds/DMSO. DMSO served as the negative control vehicle. Compounds were screened on two different plates, labelled (1) and (2). Table shows the average EC_{50} value of each hit compound.

4 Discussion

A yeast-based screening approach was successfully developed and optimized to identify six cell-permeable and potent PfPDEβ inhibitors that are worth investigating further.

Chemical structures of the six hit compounds, which demonstrate high potential as PfPDEβ inhibitors, were analyzed, as depicted in Figure 8. Although all of the compounds feature a ring structure with carbon, hydrogen, nitrogen, sulfur (except BC8-8) and oxygen

(except BC11-29) atoms, along with at least one methyl group, these are common features of screening compounds. Hence, although there seems to be a resemblance between the compounds and cAMP, other chemical structural features, such as functional groups, suggest that the compounds are fairly distinct from one another and cAMP. Notably, the Tanimoto coefficient, a measure of similarity between chemical structures [41], revealed a very low value of 0.245 between the most structurally similar compounds, BC11-29 and BC42, indicating that the compounds were distinct from one another. This suggests that the hit compounds interact with the active site of PfPDEβ through different contacts.

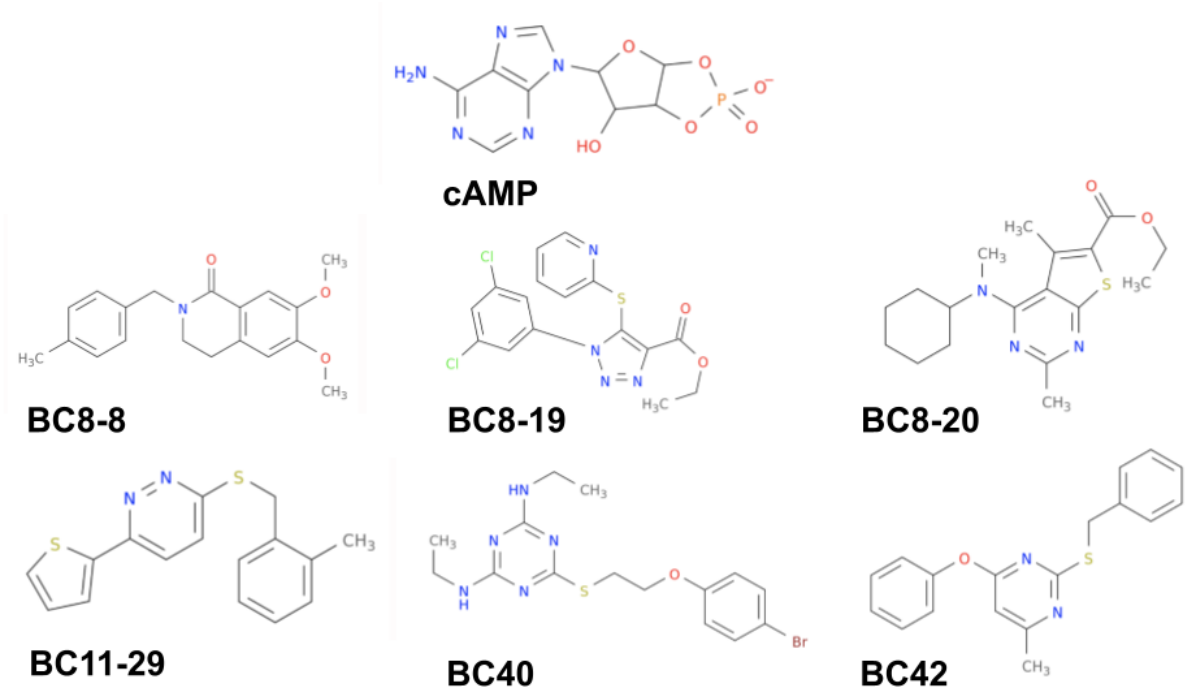

Figure 8: Chemical structures of cAMP and the six hit compounds from HTS screening.

Certain compounds in the HTS exhibited inconsistent results across the three replicates. An example is BC8-20, as indicated by the large error bars in Figure 7. In contrast, compounds like BC11-29 and BC42 demonstrated more consistent results. The observed inconsistency of BC8-20 results could potentially be attributed to solubility issues in DMSO, which can be addressed in future investigations by diluting the BC8-20 stock solution more. Furthermore, additional compounds, including BC8-22, BC11-23, BC24, BC26, and BC43,

warrant further experimentation to determine if they are hit compounds, as they showed inhibition of PfPDEβ in at least two of the assays.

In our laboratory, HTS is being performed on PfPDEα, PfPDEδ and PfPDEγ, in addition to PfPDEβ. Notably, several hit compounds identified in the PfPDEβ screens were not highly specific to PfPDEβ as they were also identified as hits in PfPDEα (unpublished, Layne Kiratsous). This finding is unsurprising considering the compounds used in the PfPDEβ screens had previously been identified as hit compounds in HsPDE screens. Hence, these compounds likely bind promiscuously to various PDEs. In contrast, BC8-8 displayed significant activity against PfPDEβ, but no activity against PfPDEα. Thus, both promiscuous and selective PfPDEβ inhibitors were identified in this study.

This study showcases the efficacy of *S. pombe*-based screening in successfully validating drug targets and identifying biologically active, potent and selective PDE inhibitors in a cost-effective and efficient manner, making it highly practical for HTS. Specifically, the compounds are accessed based on their ability to promote 5FOA-resistant growth in *S. pombe* during a 48-hour period. This implies that the identified hit compounds are cell-permeable, chemically stable and nontoxic to *S. pombe*, suggesting they can be directly tested in *P. falciparum*.

5 Future work

Further work includes the screening of hit compounds using a purified PfPDEβ enzyme *in vitro* assay to validate their inhibitory activity. Additionally, in collaboration with Manoj Duraisingh from Harvard School of Public Health, hit compounds will be used in whole *P. falciparum* parasite screens to assess whether the hit compounds can directly reduce parasite blood stage invasion and growth. If warranted, strain GKS1 can then be used in a HTS at the Broad Institute to discover compounds that could be developed into novel antimalarial drugs.

6 Conclusion

This study describes the successful cloning of the PfPDEβ gene and construction of yeast strains for the development and optimization of a yeast-based High-Throughput Screening assay. I demonstrated that PfPDEβ can be inhibited by small molecules and identified six PfPDEβ inhibitors, namely BC8-8, BC8-19, BC8-20, BC11-29, BC40, and BC42, with BC8-20 being the strongest and most potent lead compound. These compounds can be used for whole-parasite screening to evaluate the effect of inhibiting PfPDEs on *P. falciparum*, contributing to antimalarial drug discovery efforts. Additionally, my hit compound library and optimized screening conditions are resources that can be leveraged for future screens against PDEs from animals and parasites. This will deepen our understanding of PDEs and facilitate the development of novel therapies for cyclic nucleotide pathway-related diseases.

7 Acknowledgments

My sincere gratitude to Professor Charlie Hoffman for his patient guidance throughout the mentorship. Thank you to Boston College for the support and facilities. Many thanks to Indu Prakash, Catherine Xue, Peter Gaydarov, Shriya Bhat, teaching assistants, and other Research Science Institute (RSI) staff for their valuable advice. Thank you to RSI, the Center for Excellence in Education (CEE), the Massachusetts Institute of Technology (MIT), and the Ministry of Education Singapore, for this valuable opportunity and for sponsoring me this summer.

References

[1] E. Lasonder, K. More, S. Singh, et al. camp-dependent signaling pathways as potential targets for inhibition of plasmodium falciparum blood stages. *Frontiers in Microbiology*, 12:p. 684,005, 2021.

[2] W. H. Organisation. World malaria report 2022, 2022. URL `https://www.who.int/teams/global-malaria-programme/reports/world-malaria-report-2022`.

[3] R. W. Snow. Global malaria eradication and the importance of plasmodium falciparum epidemiology in africa. *BMC medicine*, 13(1):pp. 1–3, 2015.

[4] T. Muller-Reichert. *Electron microscopy of model systems*. Academic Press, 2010.

[5] S. Dini, S. Zaloumis, P. Cao, et al. Investigating the efficacy of triple artemisinin-based combination therapies for treating plasmodium falciparum malaria patients using mathematical modeling. *Antimicrobial agents and chemotherapy*, 62(11):pp. 10–1128, 2018.

[6] A. M. Dondorp, F. Nosten, P. Yi, et al. Artemisinin resistance in plasmodium falciparum malaria. *New England journal of medicine*, 361(5):pp. 455–467, 2009.

[7] E. A. Ashley, M. Dhorda, R. M. Fairhurst, et al. Spread of artemisinin resistance in plasmodium falciparum malaria. *New England Journal of Medicine*, 371(5):pp. 411–423, 2014.

[8] K. M. Tun, M. Imwong, K. M. Lwin, et al. Spread of artemisinin-resistant plasmodium falciparum in myanmar: a cross-sectional survey of the k13 molecular marker. *The Lancet infectious diseases*, 15(4):pp. 415–421, 2015.

[9] W. H. Organization, et al. Artemisinin and artemisinin-based combination therapy resistance: status report. Technical report, World Health Organization, 2016.

[10] C. Flueck, L. G. Drought, A. Jones, et al. Phosphodiesterase beta is the master regulator of camp signalling during malaria parasite invasion. *PLoS biology*, 17(2):p. e3000,154, 2019.

[11] D. A. Baker, L. G. Drought, C. Flueck, et al. Cyclic nucleotide signalling in malaria parasites. *Open biology*, 7(12):p. 170,213, 2017.

[12] A. Dawn, S. Singh, K. R. More, et al. The central role of camp in regulating plasmodium falciparum merozoite invasion of human erythrocytes. *PLoS pathogens*, 10(12):p. e1004,520, 2014.

[13] F. H. Beraldo, F. M. Almeida, A. M. da Silva, et al. Cyclic amp and calcium interplay as second messengers in melatonin-dependent regulation of plasmodium falciparum cell cycle. *The Journal of cell biology*, 170(4):pp. 551–557, 2005.

[14] L. McRobert, C. J. Taylor, W. Deng, et al. Gametogenesis in malaria parasites is mediated by the cgmp-dependent protein kinase. *PLoS biology*, 6(6):p. e139, 2008.

[15] R. W. Moon, C. J. Taylor, C. Bex, et al. A cyclic gmp signalling module that regulates gliding motility in a malaria parasite. *PLoS pathogens*, 5(9):p. e1000,599, 2009.

[16] J. Corbin. Mechanisms of action of pde5 inhibition in erectile dysfunction. *International journal of impotence research*, 16(1):pp. S4–S7, 2004.

[17] H. A. Ghofrani, J. Pepke-Zaba, J. A. Barbera, et al. Nitric oxide pathway and phosphodiesterase inhibitors in pulmonary arterial hypertension. *Journal of the American College of Cardiology*, 43(12S):pp. S68–S72, 2004.

[18] H. Ke and H. Wang. Crystal structures of phosphodiesterases and implications on substrate specificity and inhibitor selectivity. *Current topics in medicinal chemistry*, 7(4):pp. 391–403, 2007.

[19] C. J. Taylor, L. McRobert, and D. A. Baker. Disruption of a plasmodium falciparum cyclic nucleotide phosphodiesterase gene causes aberrant gametogenesis. *Molecular microbiology*, 69(1):pp. 110–118, 2008.

[20] L. Wentzinger, S. Bopp, H. Tenor, et al. Cyclic nucleotide-specific phosphodiesterases of plasmodium falciparum: Pfpdeα, a non-essential cgmp-specific pde that is an integral membrane protein. *International journal for parasitology*, 38(14):pp. 1625–1637, 2008.

[21] F. Schwach, E. Bushell, A. R. Gomes, et al. Plasmo gem, a database supporting a community resource for large-scale experimental genetics in malaria parasites. *Nucleic acids research*, 43(D1):pp. D1176–D1182, 2015.

[22] J. Inglese. Expanding the hts paradigm, 2002.

[23] P. Denny and P. Steel. Yeast as a potential vehicle for neglected tropical disease drug discovery. *Journal of Biomolecular Screening*, 20(1):pp. 56–63, 2015.

[24] P. W. Denny. Yeast: bridging the gap between phenotypic and biochemical assays for high-throughput screening. *Expert Opinion on Drug Discovery*, 13(12):pp. 1153–1160, 2018.

[25] C. S. Hoffman. Use of a fission yeast platform to identify and characterize small molecule pde inhibitors. *Frontiers in Pharmacology*, 12:p. 833,156, 2022.

[26] C. S. Hoffman. Except in every detail: comparing and contrasting g-protein signaling in saccharomyces cerevisiae and schizosaccharomyces pombe. *Eukaryotic Cell*, 4(3):pp. 495–503, 2005.

[27] F. D. Ivey, L. Wang, D. Demirbas, et al. Development of a fission yeast-based high-throughput screen to identify chemical regulators of camp phosphodiesterases. *Journal of biomolecular screening*, 13(1):pp. 62–71, 2008.

[28] A. A. Duina, M. E. Miller, and J. B. Keeney. Budding yeast for budding geneticists: a primer on the saccharomyces cerevisiae model system. *Genetics*, 197(1):pp. 33–48, 2014.

[29] J. Hill, K. Donald, D. E. Griffiths, et al. Dmso-enhanced whole cell yeast transformation. *Nucleic acids research*, 19(20):p. 5791, 1991.

[30] C. S. Hoffman. Preparation of yeast dna. *Current protocols in molecular biology*, 39(1):pp. 13–11, 1997.

[31] J. Lederberg and E. M. Lederberg. Replica plating and indirect selection of bacterial mutants. *Journal of bacteriology*, 63(3):pp. 399–406, 1952.

[32] D. Bajusz, A. Rácz, and K. Héberger. Why is tanimoto index an appropriate choice for fingerprint-based similarity calculations? *Journal of cheminformatics*, 7(1):pp. 1–13, 2015.

[33] D. A. Kelly and C. S. Hoffman. Gap repair transformation in fission yeast to exchange plasmid-selectable markers. *Biotechniques*, 33(5):pp. 978–982, 2002.

[34] M. Jin, M. Fujita, B. M. Culley, et al. sck1, a high copy number suppressor of defects in the camp-dependent protein kinase pathway in fission yeast, encodes a protein homologous to the saccharomyces cerevisiae sch9 kinase. *Genetics*, 140(2):pp. 457–467, 1995.

[35] C. Xu, A. R. Wyman, M. A. Alaamery, et al. Anti-inflammatory effects of novel barbituric acid derivatives in t lymphocytes. *International immunopharmacology*, 38:pp. 223–232, 2016.

[36] M. A. Alaamery, A. R. Wyman, F. D. Ivey, et al. New classes of pde7 inhibitors identified by a fission yeast-based hts. *Journal of biomolecular screening*, 15(4):pp. 359–367, 2010.

[37] O. Ceyhan, K. Birsoy, and C. S. Hoffman. Identification of biologically active pde11-selective inhibitors using a yeast-based high-throughput screen. *Chemistry & biology*, 19(1):pp. 155–163, 2012.

[38] D. Demirbas, O. Ceyhan, A. R. Wyman, et al. Use of a schizosaccharomyces pombe pka-repressible reporter to study cgmp metabolising phosphodiesterases. *Cellular signalling*, 23(3):pp. 594–601, 2011.

[39] D. Demirbas, A. R. Wyman, M. Shimizu-Albergine, et al. A yeast-based chemical screen identifies a pde inhibitor that elevates steroidogenesis in mouse leydig cells via pde8 and pde4 inhibition. *PLoS One*, 8(8):p. e71,279, 2013.

[40] J. Ferreira and A. Zwinderman. On the benjamini–hochberg method. 2006.

[41] P. Willett and V. Winterman. A comparison of some measures for the determination of inter-molecular structural similarity measures of inter-molecular structural similarity. *Quantitative Structure-Activity Relationships*, 5(1):pp. 18–25, 1986.

A Appendix

A.1 Life Cycle of *Plasmodium falciparum*

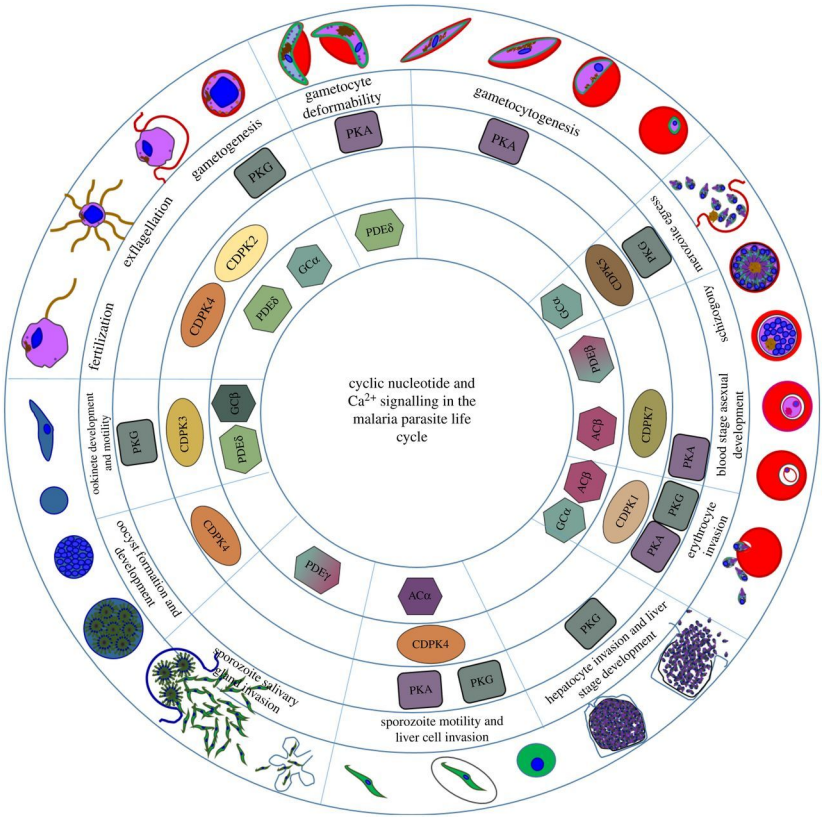

Supplementary Figure 1: Life cycle of *Plasmodium falciparum* illustrating the specific stages and their respective cyclic nucleotide signaling components and protein kinases (from Baker, D. A., Drought, L. G., Flueck, C., Nofal, S. D., Patel, A., Penzo, M., & Walker, E. M. (2017). Cyclic nucleotide signalling in malaria parasites. Open biology, 7(12), 170213. https://doi.org/10.1098/rsob.170213 [11])

A.2 PDE Specificity

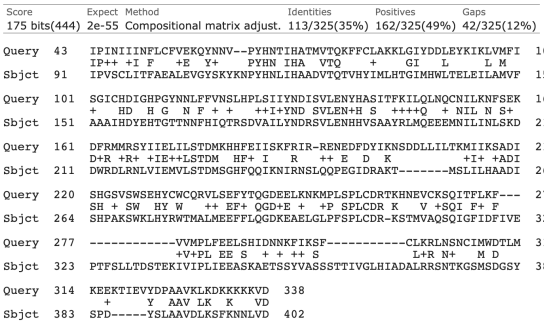

```
 Score          Expect  Method                          Identities          Positives           Gaps
 175 bits(444)  2e-55   Compositional matrix adjust.    113/325(35%)        162/325(49%)        42/325(12%)

Query  43   IPINIIINFLCFVEKQYNNV--PYHNTIHATMVTQKFFCLAKKLGIYDDLEYKIKLVMFI  100
            IP++ +I F    +E  Y+     PYHN IHA  VTQ    +     GI    L     L M
Sbjct  91   IPVSCLITFAEALEVGYSKYKNPYHNLIHAADVTQTVHYIMLHTGIMHWLTELEILAMVF  150

Query  101  SGICHDIGHPGYNNLFFVNSLHPLSIIYNDISVLENYHASITFKILQLNQCNILKNFSEK  160
            +   HD  H G  N F + +   ++I+YND SVLEN+H S  ++++Q  + NIL N S+
Sbjct  151  AAAIHDYEHTGTTNNFHIQTRSDVAILYNDRSVLENHHVSAAYRLMQEEEMNILINLSKD  210

Query  161  DFRMMRSYIIELILSTDMKHHFEIISKFRIR-RENEDFDYIKNSDDLLILTKMIIKSADI  219
            D+R +R+ +IE++LSTDM  HF+ I   R   ++ E  D  K          +I+ +ADI
Sbjct  211  DWRDLRNLVIEMVLSTDMSGHFQQIKNIRNSLQQPEGIDRAKT-------MSLILHAADI  263

Query  220  SHGSVSWSEHYCWCQRVLSEFYTQGDEELKNKMPLSPLCDRTKHNEVCKSQITFLKF---  276
            SH + SW  HY W   ++ EF+ QGD+E +  +P SPLCDR K   V +SQI F+ F
Sbjct  264  SHPAKSWKLHYRWTMALMEEFFLQGDKEAELGLPFSPLCDR-KSTMVAQSQIGFIDFIVE  322

Query  277  ------------VVMPLFEELSHIDNNKFIKSF-----------CLKRLNSNCIMWDTLM  313
                        +V+PL EE S  + + ++ S             L+R N+   M D
Sbjct  323  PTFSLLTDSTEKIVIPLIEEASKAETSSYVASSSTTIVGLHIADALRRSNTKGSMSDGSY  382

Query  314  KEEKTIEVYDPAAVKLKDKKKKKVD  338
              +     Y  AAV LK  K   VD
Sbjct  383  SPD-----YSLAAVDLKSFKNNLVD  402
```

(a) Protein BLAST alignment of PfPDEβ and HsPDE1A

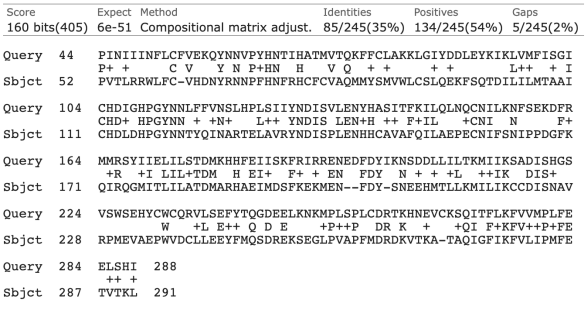

```
 Score          Expect  Method                          Identities          Positives           Gaps
 160 bits(405)  6e-51   Compositional matrix adjust.    85/245(35%)         134/245(54%)        5/245(2%)

Query  44   PINIIINFLCFVEKQYNNVPYHNTIHATMVTQKFFCLAKKLGIYDDLEYKIKLVMFISGI  103
            P+ +     C V   Y N P+HN  H   V Q  + +     + +       L++  + I
Sbjct  52   PVTLRRWLFC-VHDNYRNNPFHNFRHCFCVAQMMYSMVWLCSLQEKFSQTDILILMTAAI  110

Query  104  CHDIGHPGYNNLFFVNSLHPLSIIYNDISVLENYHASITFKILQLNQCNILKNFSEKDFR  163
            CHD+ HPGYNN + +N+    L++ YNDIS LEN+H ++ F+IL   +CNI  N     F+
Sbjct  111  CHDLDHPGYNNTYQINARTELAVRYNDISPLENHHCAVAFQILAEPECNIFSNIPPDGFK  170

Query  164  MMRSYIIELILSTDMKHHFEIISKFRIRRENEDFDYIKNSDDLLILTKMIIKSADISHGS  223
             +R  +I LIL+TDM  H EI+  F+ + EN  FDY  N + + +L  ++IK  DIS+
Sbjct  171  QIRQGMITLILATDMARHAEIMDSFKEKMEN--FDY-SNEEHMTLLKMILIKCCDISNAV  227

Query  224  VSWSEHYCWCQRVLSEFYTQGDEELKNKMPLSPLCDRTKHNEVCKSQITFLKFVVMPLFE  283
                  W   +L E++ Q D E    +P++P  DR K  +   +QI F+KFV++P+FE
Sbjct  228  RPMEVAEPWVDCLLEEYFMQSDREKSEGLPVAPFMDRDKVTKA-TAQIGFIKFVLIPMFE  286

Query  284  ELSHI  288
              ++ +
Sbjct  287  TVTKL  291
```

(b) Protein BLAST alignment of PfPDEβ and HsPDE9A

Supplementary Figure 2: Amino acid sequence of PfPDEβ is significantly different from that of HsPDEs.

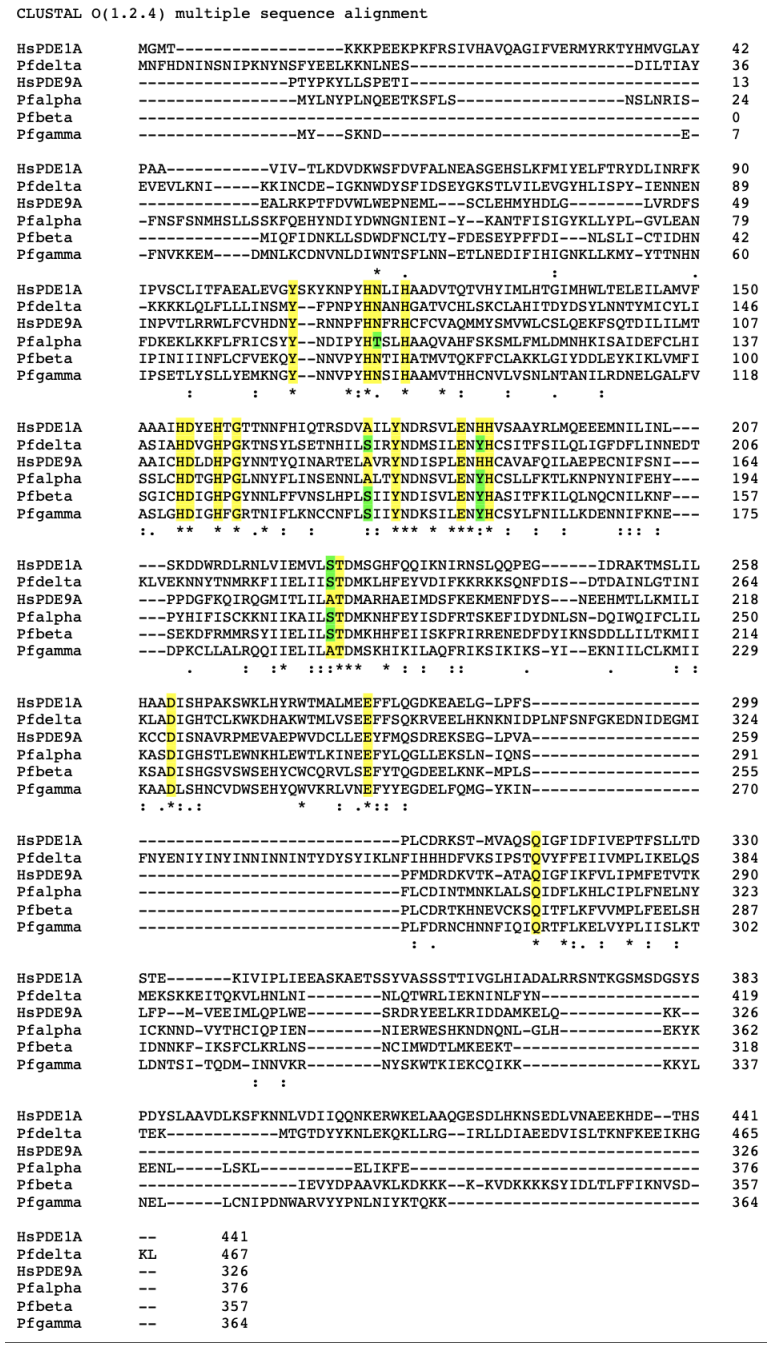

Supplementary Figure 3: Clustal Omega alignment of HsPDEs and PfPDEβ. Of the 18 invariant amino acids in HsPDEs (highlighted in yellow), PfPDEβ has 3 different amino acids (highlighted in green).

A.3 Oligonucleotides

Name	Genotype
Tif-rev	GGGTTTTCCCAGTCACGACG
ura5-seq	TTTAATATTCGGTGGTCTCTTCAG

Supplementary Table 1: Oligonucleotides used in this study.

A.4 Compound Collection Library

Collection	Compounds
1	DMSO Roli BC12 BC13 BC14 BC18 BC20 BC21 BC22 BC23 BC24 BC25 BC26 BC27 BC28 BC29 BC30 BC31 BC32 BC33 BC34 BC35
2	DMSO BC37 BC38 BC39 BC40 BC41 BC42 BC43 BC44 BC45 BC46 BC47 BC48 BC49 BC50 BC51 BC52 BC53 BC54 BC55 BC56 BC57
3	DMSO BC58 BC58-3 BC61 BC63 BC64 BC65 BC66 BC67 BC68 BC69 BC69-3 BC70 BC71 BC72 BC73 BC74 BC75 BC76 BC77 BC26-2 BC26-3
4	DMSO BC11-1 BC11-2 BC11-3 BC11-4 BC11-5 BC11-6 BC11-8 BC11-8-2 BC11-9 BC11-10 BC11-11 BC11-12 BC11-13 BC11-14 BC11-15 BC11-17 BC11-18 BC-19 BC11-20 BC11-21 BC11-22
5	DMSO BC11-23 BC11-24 BC11-25 BC11-26 BC11-27 BC11-28 BC11-29 BC11-30 BC11-31 BC11-32 BC11-33 BC11-34 BC11-35 BC11-36 BC11-37 BC11-38 BC8-1 BC8-2 BC8-3 BC8-4 BC8-5
6	DMSO BC8-6 BC8-7 BC8-8 BC8-9 BC8-10 BC8-11 B08-12 BC8-13 BC8-14 BC8-15 BC8-16 BC8-17 BC8-18 BC8-19 BC8-20 BC8-21 BC8-22 BC8-23 BC8-24 BC8-25 BC8-26
7	DMSO BC8-27 BC8-28 BC8-1A BC8-1B BC8-1C BC8-1D BC8-1E BC8-1F BC8-1G BC8-1H BC8-5A BC8-5B BC8-5C BC8-A1 BC8-A2 BC8-A3 BC8-A4 BC8-A5 BC8-A6 BC8-A7 BC8-A8
8	DMSO BC8-A9 BC8-A10 BC8-A11 BC69-1 BC69-2 BC69-3 BC69-4 BC69-5 BC69-6 BC8-BB BC8-23C BC8-15C Tadalfil BRL50481 Zaprinast BC24 BC26 BC58 BC11-21 BC8-19 BC8-22

Supplementary Table 2: 162-compound collection used for screening.

Collection	Compounds
Focus-1	DMSO BC14 BC39 BC40 BC41 BC42 BC43 BC44 BC51 BC52 BC56 BC58 BC11-18 BC11-23 BC11-25 BC11-26 BC11-27 BC11-28 BC11-29 BC11-31 BC11-32 BC11-34
Focus 2	DMSO BC11-35 BC11-36 BC11-37 BC11-38 BC8-1 BC8-2 BC8-3 BC8-8 BC8-9 BC8-12 BC8-20 BC8-21 BC8-22 BC8-26 BC69-2 BC69-6 BC8-23C BC8-15C BRL50481 BC24 BC8-19

Supplementary Table 3: 42-compound focused collection used for screening.

A.5 Plasmid transformation in *S. pombe*

Strains CHP1236 and CHP1247 were cultured overnight in YES and EMM respectively. Then, strains were subcultured into 30ml EMM for five hours to target for 10^7 cells/ml. Using a tabletop centrifuge, cells were pelleted and washed with an equal volume of sterile water. Cells were pelleted again, brought up in 1ml water and then transferred to an Eppendorf tube. Cells were pelleted for five seconds and washed with 1ml 1x LiOAc/TE buffer solution (2ml 10x LiOAc (1M, pH 7.5), 2ml 10x TE, 16ml sterile water). Cells were pelleted again and brought to 2x10^9 cells/ml in 150μl 1x LiOAc/TE. 3μl of 10mg/ml boiled carrier DNA was added to cells and incubated at room temperature for 10 minutes. Then, 390μl of 40% PEG in 1x LiOAc/TE (2ml 10x LiOAc, 2ml 10x TE, 8g PEG (3350), 9.75ml sterile water (boiled for 6-10 minutes)) was added and incubated at 30℃. 90μl of transformation mix was transferred into a tube containing the 1μl *Pst*I cut plasmid and incubated for two hours at 30℃. After adding 10.75μl of DMSO, the mixture was heat shocked for five minutes at 42℃. Cells were plated onto an EMM-lys plate to select for transformants. Transformants were subjected to PCR with oligonucleotides Tif-rev and ura5-seq (Supp. Table 1) followed by gel electrophoresis.

A.6 Plasmid Rescue

Cells were collected from EMM-lys plate into a 1.5ml Eppendorf tube. 0.2ml of Smash and Grab buffer (10ml 1% SDS, 2.0ml 2% Triton X-100, 2ml 100mM NaCl, 1ml 10mM

Tris (pH 8.0), 0.2ml 1mM EDTA (pH 8.0), 84.8ml sterile water), 0.3g acid-washed glass beads and 0.2ml phenol-chloroform were added into the tube. The mixture was vortexed for four minutes and pelleted for five minutes in a microfuge. 40μl of the aqueous layer was transferred into a new tube containing 40μl isopropanol and placed on ice for 30 minutes. The mixture was pelleted for 10 minutes in a microfuge and the liquid was removed. 200μl of 70% ethanol was added and the mixture was placed on ice for another 10 minutes. Ethanol was removed and the pellet was dried in a Speedvac and resuspended in 10μl of sterile water. 1.0μl DNA used to transform *Escherichia coli (E.coli)* ElectroTen Blue cells to ampicillin resistance by electroporation (2250V, 200Ω, 25 microfarad at a time constant of 4.5ms). Cells were collected into 1ml Luria-Bertani (LB) liquid and grown for 60 minutes at 37℃. Cells were pelleted for seven minutes at 4000RPM and liquid was removed. Cells were resuspended in 100μl of remaining medium and spread to an LB ampicillin (Amp) plate to select for transformants.